A New Approach to the Spectral Study of Unstable Radicals and Ions in Solution by the Use of an Inert Gas Glovebox System: Observation and Analysis of the Infrared Spectra of the Radical Anion and Dianion of *p*-Terphenyl

Akira Sakamoto,* Tomohisa Harada, and Naoko Tonegawa

Materials Science Division, Graduate School of Science and Engineering, Saitama University, Shimo-okubo 255, Sakura-ku, Saitama 338-8570, Japan

Received: July 8, 2007; In Final Form: October 1, 2007

By using a Fourier-transform infrared spectrometer contained in an inert gas glovebox system (oxygen and water concentrations: <0.1 ppm), high-quality infrared absorption spectra have been observed for the radical anion and dianion of *p*-terphenyl in tetrahydrofuran solutions. Density functional theory with the B3LYP nonlocal exchange-correlation functional and the 6-311+G** basis set has been used for the calculations of the structures and infrared spectra of the neutral species, radical anion, and dianion of *p*-terphenyl. The observed infrared spectra of the radical anion and dianion are in good agreement with those calculated by density functional theory. The origin of the strong infrared absorption intensities characteristic of the radical anion and dianion are discussed in terms of changes in electronic structures induced by specific normal vibrations (electron−molecular vibration interaction).

1. Introduction

In conducting charge-transfer complexes, conducting polymers, and some kinds of biological systems, electron transport is supported by ionic species of molecules, whose structures are different from those of neutral species. Since vibrational spectra are sensitive to changes in molecular structures, vibrational spectroscopy is considered to be useful for studying structural characteristics of ionic species and electron transport in these systems.[1−3]

Conjugated conducting polymers such as poly(*p*-phenylene) have attracted much attention from both fundamental and practical viewpoints because of their interesting physical properties.[4] To understand the optical and electrical properties of nondegenerate conjugated polymers such as poly(*p*-phenylene), polarons[5−7] and bipolarons[6−8] are proposed as elementary excitations. A negative (positive) polaron and a negative (positive) bipolaron correspond, respectively, to a radical anion (radical cation) and a dianion (dication) which extend over a certain number of repeating units.

Since the radical ions and divalent ions of oligomers can be considered to be good models of polarons and bipolarons in doped conducting polymers, quantum chemical calculations for the radical ions and divalent ions of *p*-oligophenyls have been carried out at various theoretical levels for studying polarons and bipolarons in doped poly(*p*-phenylene).[9−17] Experimentally, Furukawa et al.[18,19] have analyzed the Raman spectra of Na-doped poly(*p*-phenylene) on the basis of the Raman spectra of the radical anions and dianions of *p*-oligophenyls and have concluded that negative polarons and bipolarons are generated in Na-doped poly(*p*-phenylene). In ref 18, the Raman spectra of the radical anions and dianions of *p*-oligophenyls (*p*-terphenyl to *p*-sexiphenyl) were measured successfully, because the Raman measurements were possible for solutions in a completely sealed glass apparatus. Alternatively, the infrared absorption spectra of the radical ions and divalent ions of *p*-oligophenyls have not yet been reported, with the exception of a work on infrared measurements of the radical anion of biphenyl by the use of mid-infrared optical fibers.[20]

Efforts have been made to measure reliable and high-quality infrared absorption spectra of organic radical ions and divalent ions produced by various methods such as chemical reactions,[20−26] electrochemical technique,[27] electron bombardments,[28−34] vacuum ultraviolet photolyses,[35−38] pulsed-glow discharge,[39,40] X-ray irradiation,[41] and low-temperature co-deposits with alkali metals,[42,43] and so forth. However, it is not easy to observe the infrared spectra of radical ions and divalent ions, because they are generally unstable at room temperature and in the air. In particular, reliable infrared spectra of only a small number of anionic species with conjugated π-electrons have been measured,[20−24,26,27,33] whereas the infrared spectra have been measured for the cationic species of many polycyclic aromatic hydrocarbons (PAHs) in the matrix-isolated condition.[28−38] This is partly because radical anions and dianions are very sensitive to molecular oxygen and water, and partly because many radical anions and dianions are intrinsically unstable in the isolated state.

In the present study, we have used a new approach to the spectral study of unstable radical and ionic species in solution by the use of an inert gas glovebox system, in which the oxygen and water concentrations are less than 0.1 ppm. We have obtained high-quality infrared and electronic absorption spectra of radical anion (charge: $-e$, spin: 1/2) and dianion (charge: $-2e$, spin: 0) of *p*-terphenyl in solutions by using a Fourier-transform infrared spectrometer and an ultraviolet and visible spectrometer contained in an inert gas glovebox system. The observed infrared spectra have been analyzed on the basis of density functional theory calculations at the B3LYP (Becke's three-parameter hybrid method[44] using the Lee−Yang−Parr correlation functional[45]) level. Some specific vibrational modes

* To whom correspondence should be addressed. Fax: +81-48-858-9473. E-mail: sakamoto@chem.saitama-u.ac.jp.

10.1021/jp075304n CCC: $40.75
Published on Web 01/17/2008

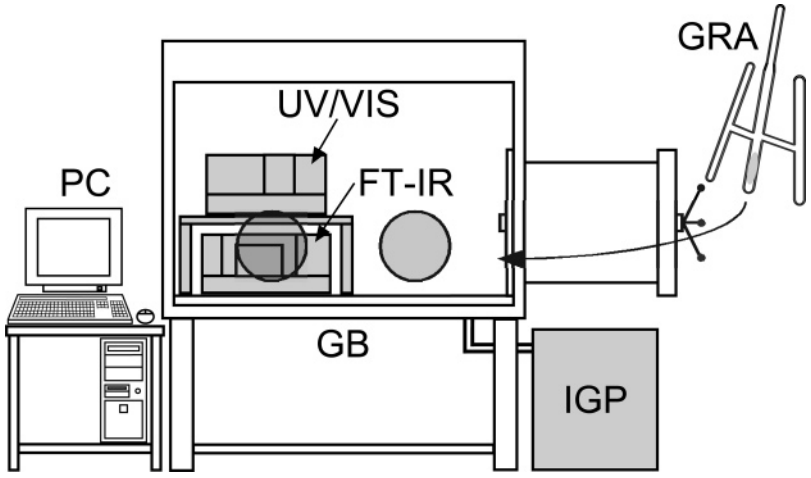

Figure 1. Schematic diagram of the experimental setup for infrared and electronic absorption measurements using a Fourier-transform infrared spectrometer and an ultraviolet and visible spectrometer in an inert gas globebox system. GB: glovebox, IGP: inert gas purification system, FT−IR: Fourier-transform infrared spectrophotometer, UV−VIS: ultraviolet and visible spectrophotometer, GRA: glass reaction apparatus, PC: personal computer.

of the radical anion and dianion have extremely large infrared absorption intensities. The mechanism that gives rise to the large infrared intensities for such vibrations is discussed.

2. Experimental Section

The experimental setup for infrared and electronic absorption measurements using a Fourier-transform infrared spectrometer and an ultraviolet and visible spectrometer contained in an inert gas glovebox system is shown schematically in Figure 1. Infrared spectra were recorded at room temperature on a Fourier-transform infrared spectrophotometer (JASCO FT-IR 4100) in the glovebox system. Interferograms were accumulated at 100 times and averaged to obtain a satisfactory signal-to-noise ratio. The wavenumber resolution was 4 cm^{-1}. Electronic absorption spectra were measured on an ultraviolet and visible spectrophotometer (JASCO V-530) in the glovebox system.

The degassed and anhydrous tetrahydrofuran (d_8-THF and h_8-THF) solutions of neutral *p*-terphenyl were prepared using a vacuum system and introduced in the glovebox system. The radical anion and dianion of *p*-terphenyl were prepared by bringing their neutral solutions into contact with a sodium mirror in the glovebox system. The progress of the reduction reaction was controlled by the time of contact between the solution and the sodium mirror, and was monitored by measuring electronic absorption spectra. After the formation of the radical anion and dianion of *p*-terphenyl was confirmed by their electronic absorption spectra, their THF solutions were transferred to a CaF_2 cell (BioTools BioCell) with an optical path length of 123 μm. The infrared and electronic absorption spectra of the radical anion and dianion of *p*-terphenyl were obtained from such THF solutions in a CaF_2 cell.

The structures and vibrational properties (harmonic frequencies, vibrational patterns, and infrared intensities) were calculated for the neutral species, radical anion (charge: $-e$, spin multiplicity: 2), and dianion (charge: $-2e$, spin multiplicity: 1) of *p*-terphenyl. Counterions were not included in the calculations for the radical anion and dianion. Density functional theory calculations at the B3LYP (Becke's three-parameter hybrid method[44] using the Lee−Yang−Parr correlation functional[45]) level in combination with the 6-311+G** basis set were performed by using the GAUSSIAN 03 program.[46] The "UltraFine" grid was used for numerical calculations of two-electron integrals.

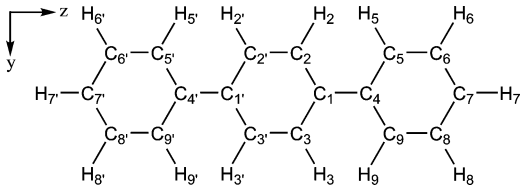

Figure 2. Numbering of atoms and the Cartesian coordinate system for *p*-terphenyl.

Since *p*-terphenyl has three benzene rings and two inter-ring C−C bonds (Figure 2), geometry optimizations for the neutral species, radical anion, and dianion of *p*-terphenyl were performed for two possible conformers: one with a helical conformation (D_2 symmetry, gauche$^+$−gauche$^+$ with respect to the two inter-ring C−C bonds) and the other with an alternately twisted conformation (C_{2h} symmetry, gauche$^+$−gauche$^-$). An almost planar structure was obtained for the dianion of *p*-terphenyl and, therefore, the geometry optimization of this species was finally performed under D_{2h} symmetry. No imaginary frequency mode was found at the optimized structures of all the species. The calculated wavenumbers are multiplied by a single scale factor of 0.9751 for the helical radical anion, 0.9758 for the twisted radical anion, and 0.9759 for the dianion, each of which was determined to obtain the best fit between the calculated wavenumbers and the observed wavenumbers. Calculated atomic displacements in each vibrational mode were depicted with the VLX program.[47]

3. Results and Discussion

3.1. Molecular Structures. The numbering of atoms in *p*-terphenyl is shown in Figure 2. The structural parameters calculated at the B3LYP/6-311+G** level for the neutral species, radical anion, and dianion of *p*-terphenyl are listed in Table 1. The density functional theory calculations have shown that *p*-terphenyl in the neutral state has two conformations around two inter-ring C−C bonds: a helical structure (D_2 symmetry) and an alternately twisted structure (C_{2h} symmetry). The calculated energy difference between the two conformers is 60.7 J mol^{-1} (14.5 cal mol^{-1}) and the twisted structure is slightly more stable than the helical structure. The calculated values of the torsional angles around the inter-ring C_1-C_4 and $C_{1'}-C_{4'}$ bonds in the helical structure are +40.0 and +40.0°,

TABLE 1: Structural Parameters Calculated at the B3LYP/6-311+G Level for the Neutral Species, Radical Anion, and Dianion of *p*-Terphenyl**

	bond lengths /Å and angles/ deg				
	neutral		radical anion		dianion
	helical	twisted	helical	twisted	planar
$\tau(C_2C_1C_4C_5)$	+40.0	+39.5	+9.0	+12.8	0.0
$\tau(C_{2'}C_{1'}C_{4'}C_{5'})$	+40.0	−39.5	+9.0	−12.8	0.0
$r(C_1C_2)$, $r(C_1C_3)$	1.402	1.402	1.427	1.427	1.447
$r(C_2C_{2'})$, $r(C_3C_{3'})$	1.390	1.390	1.378	1.378	1.372
$r(C_1C_4)$	1.484	1.484	1.450	1.450	1.418
$r(C_4C_5)$, $r(C_4C_9)$	1.403	1.403	1.427	1.426	1.451
$r(C_5C_6)$, $r(C_8C_9)$	1.392	1.392	1.387	1.387	1.382
$r(C_6C_7)$, $r(C_7C_8)$	1.394	1.394	1.402	1.402	1.414
$r(C_2H_2)$	1.084	1.084	1.084	1.085	1.086
$r(C_5H_5)$	1.084	1.084	1.083	1.083	1.085
$r(C_6H_6)$	1.084	1.084	1.087	1.087	1.091
$r(C_7H_7)$	1.084	1.084	1.084	1.084	1.086
$\theta(C_2C_1C_3)$	117.6	117.6	114.3	114.5	112.8
$\theta(C_1C_2C_{2'})$	121.2	121.2	122.8	122.8	123.6
$\theta(C_5C_4C_9)$	118.1	118.1	115.1	115.2	113.3
$\theta(C_4C_5C_6)$	121.0	121.0	122.3	122.2	122.9
$\theta(C_5C_6C_7)$	120.3	120.3	121.3	121.3	122.3
$\theta(C_6C_7C_8)$	119.4	119.4	117.7	117.8	116.3
$\theta(C_1C_2H_2)$	119.5	119.5	119.7	119.5	119.2
$\theta(C_4C_5H_5)$	119.5	119.5	119.5	119.4	119.1
$\theta(C_5C_6H_6)$	119.7	119.7	119.0	119.0	118.4
$\theta(C_6C_7H_7)$	120.3	120.3	121.1	121.1	121.8

respectively, and those of the twisted structure are +39.5 and −39.5°, respectively. Similar two conformers have been calculated at the BLYP/6-31G* and B3LYP/6-311+G** levels.[17,48] X-ray and neutron diffraction studies[49−51] have shown that *p*-terphenyl exhibits a nearly planar structure in the crystalline state at room temperature, whereas it takes a twisted structure in the crystalline state below 193 K. In the gaseous state, it has been reported that *p*-terphenyl takes a twisted structure.[52] Recently, the infrared and Raman spectra observed in solution and in the melt have been explained by the coexistence of the helical and twisted conformers, on the basis of the density functional theory calculations.[48]

The density functional theory calculations have also shown that there exist two conformers for the radical anion: a helical structure (D_2 symmetry) and an alternately twisted structure (C_{2h} symmetry). The calculated energy of the twisted structure is lower than that of the helical structure by 279.4 J mol^{-1} (66.8 cal mol^{-1}). The calculated values of the torsional angles around the C_1-C_4 and $C_{1'}-C_{4'}$ bonds in the helical structure are +9.0 and +9.0°, respectively, and those of the twisted structure are +12.8 and −12.8°, respectively. These values of the torsional angles calculated for the radical anions are smaller than those for the neutral molecule. In contrast to the neutral molecule and radical anion, the calculated structure of the dianion is planar (D_{2h} symmetry). The planar structure of the dianion of *p*-terphenyl has been also obtained by the calculation at the BLYP/6-31G* level.[17]

As shown in Table 1, the $C_2-C_{2'}$ ($C_3-C_{3'}$), C_1-C_4, and C_5-C_6 (C_8-C_9) bonds are shortened and the C_1-C_2 (C_1-C_3), C_4-C_5 (C_4-C_9), and C_6-C_7 (C_7-C_8) bonds are lengthened upon going from the neutral molecule to the radical anion and from the radical anion to the dianion. The shortening of the inter-ring C_1-C_4 and $C_{1'}-C_{4'}$ bonds is closely associated with the increase in planarity upon going from the neutral molecule to the radical anion and from the radical anion to the dianion, mentioned above. It can be concluded that the addition of one and two electrons to *p*-terphenyl leads to changes from a benzenoid structure to a quinoid structure, and the changes upon going from the neutral species to the dianion are larger than those occurring from the neutral species to the radical anion. These structural changes upon going from the neutral molecule to the radical anion and from the radical anion to the dianion can be understood qualitatively from the character of the lowest unoccupied molecular orbital (LUMO) of neutral *p*-terphenyl, which is considered to be occupied with one and two electrons in the radical anion and dianion, respectively. The calculated LUMO of neutral *p*-terphenyl was antibonding for the C_1-C_2 (C_1-C_3), C_4-C_5 (C_4-C_9), and C_6-C_7 (C_7-C_8) bonds, and bonding for the $C_2-C_{2'}$ ($C_3-C_{3'}$), C_1-C_4, and C_5-C_6 (C_8-C_9) bonds. Therefore, when neutral *p*-terphenyl is reduced to the radical anion and dianion, the bonds where the LUMO is antibonding become longer and those where the LUMO is bonding become shorter. Similar structural changes have been calculated at the BLYP/6-31G* level.[17]

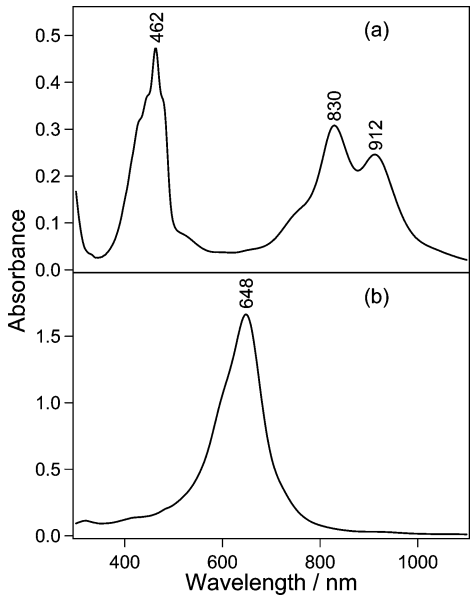

Figure 3. Electronic absorption spectra of the (a) radical anion and (b) dianion of *p*-terphenyl in THF solutions.

Other significant changes are found in the calculated bond angles of the radical anion and dianion. In particular, both the $C_2-C_1-C_3$ and $C_5-C_4-C_9$ angles are reduced by 4.8° upon going from the neutral species to the dianion. These changes may be due to the repulsion between $H_2\cdots H_5$ and $H_3\cdots H_9$ in the planar structure of the dianion.

3.2. Electronic Absorption Spectra of the Radical Anion and Dianion of *p*-Terphenyl. Electronic absorption spectra of the radical anion and dianion of *p*-terphenyl in THF solutions are shown in Figure 3, parts a and b, respectively. The THF solution of *p*-terphenyl, which was originally colorless, became green shortly after it was brought into contact with the sodium mirror. At this stage, the solution showed electronic absorption bands with their peaks at 462, 830, and 912 nm (Figure 3a). After sufficiently long contact with the sodium mirror, the solution turned blue, and the absorption maximum was observed at 648 nm (Figure 3b). The electronic absorption spectra at the above two stages (Figure 3, parts a and b) closely resemble, respectively, those of the radical anion and dianion of *p*-terphenyl reported by Balk et al.[53] These similarities indicate that the first-stage (green) solution (Figure 3a) contains the radical anion and the second-stage (blue) solution (Figure 3b) the dianion.

It is worth pointing out that the concentrations of the radical anion and dianion in THF solutions used for the electronic and infrared absorption measurements can be determined, because

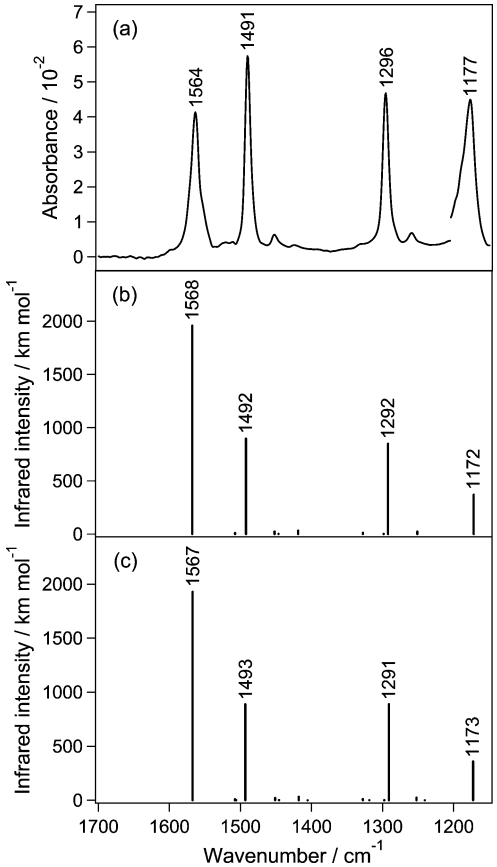

Figure 4. (a) Observed infrared spectrum of the *p*-terphenyl radical anion in THF solutions and the infrared spectra of the (b) alternately twisted and (c) helical structures of the *p*-terphenyl radical anions calculated at the B3LYP/6-311+G** level.

the molar absorption coefficients of the electronic absorption bands of the radical anion and dianion of *p*-terphenyl have been reported.[53] Using the reported molar absorption coefficients (~28 200 mol^{-1} dm^3 cm^{-1} for the 462-nm band of the radical anion and ~80 900 mol^{-1} dm^3 cm^{-1} for the 648-nm band of the dianion),[53] we calculated that the concentrations of the radical anion in THF solution in Figure 3a and the dianion in Figure 3b were 1.36×10^{-3} and 1.67×10^{-3} mol dm^{-3}, respectively. Since the both electronic and infrared absorption measurements were carried out for the identical solutions, we can also determine the molar absorption coefficients of the infrared absorption bands of the radical anion and dianion of *p*-terphenyl on the basis of the concentrations obtained from the electronic absorption measurements.

3.3. Infrared Absorption Spectra of the Radical Anion and Dianion of *p*-Terphenyl. The infrared absorption spectrum obtained from a 1.36×10^{-3} mol dm^{-3} solution of *p*-terphenyl radical anion is shown in Figure 4a. In this figure, bands due to the solvent (d_8-THF or h_8-THF) are already subtracted. The infrared absorption bands arising from the *p*-terphenyl radical anion were observed at 1564, 1491, 1296, and 1177 cm^{-1} (Figure 4a). The infrared spectra of the *p*-terphenyl radical anions calculated at the B3LYP/6-311+G** level for the alternately twisted and helical structures are shown in Figure 4, parts b and c, respectively. The calculated spectra of the twisted and helical structures (Figure 4, parts b and c) reproduce reasonably well the observed infrared spectrum (Figure 4a). Since the calculated spectra (Figure 4, parts b and c) closely resemble each other, it is not possible in the present study to determine whether the *p*-terphenyl radical anion in solution takes the twisted and/or helical conformation.

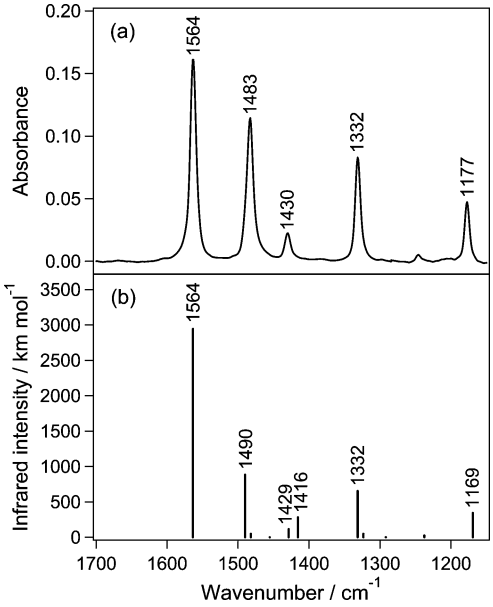

Figure 5. (a) Observed infrared spectrum of the *p*-terphenyl dianion in THF solutions and (b) the infrared spectrum of the *p*-terphenyl dianion calculated at the B3LYP/6-311+G** level.

The infrared absorption spectrum obtained from a 1.67×10^{-3} mol dm^{-3} solution of *p*-terphenyl dianion is shown in Figure 5a. In Figure 5a, bands due to the solvent (d_8-THF or h_8-THF) are already subtracted. The infrared bands arising from the dianion were observed at 1564, 1483, 1430, 1332, and 1177 cm^{-1} (Figure 5a). The infrared spectrum of the *p*-terphenyl dianion calculated at the B3LYP/6-311+G** level is shown in Figure 5b. The observed infrared spectrum (Figure 5a) agrees well with the calculated spectrum (Figure 5b). The spectral patterns of the observed and calculated infrared spectra of the *p*-terphenyl dianion (Figure 5) are similar to those of the radical anion (Figure 4), as a whole. In contrast to this similarity, the spectral patterns of the infrared spectra of the radical anion and dianion are quite different from that of the neutral molecule (not shown).

As mentioned above, we can determine the molar absorption coefficients of the infrared absorption bands of the radical anion and dianion of *p*-terphenyl on the basis of the concentrations obtained from the electronic absorption measurements. The molar absorption coefficient of the most intense infrared absorption band of the radical anion at 1491 cm^{-1} is 3430 mol^{-1} dm^3 cm^{-1}, and that of the dianion at 1564 cm^{-1} is 7820 mol^{-1} dm^3 cm^{-1}. Generally speaking, infrared bands with molar absorption coefficients larger than 200 mol^{-1} dm^3 cm^{-1} are referred to as "very strong".[54] For example, the molar absorption coefficients of C=O stretching bands of carbonyl compounds, which are well-known as very strong infrared bands, have been reported to be 300−1500 mol^{-1} dm^3 cm^{-1}.[54] Therefore, it is evident that the infrared intensities of some vibrational modes of the radical anion and dianion are extremely large.

The calculated atomic displacements for some of the a_u modes with strong intensities of the *p*-terphenyl radical anion with the alternately twisted conformation (C_{2h} symmetry) are shown in Figure 6a−d. Since the calculated atomic displacements for the b_1 modes with strong intensities of the helical conformer (D_2 symmetry) of the radical anion are almost the same as those of the twisted conformer (C_{2h} symmetry) (Figure 6a−d), they are not shown. Figure 6e−h shows the calculated atomic displacements for some of the b_{1u} modes of the *p*-terphenyl dianion (D_{2h} symmetry), which give rise to strong infrared intensities.

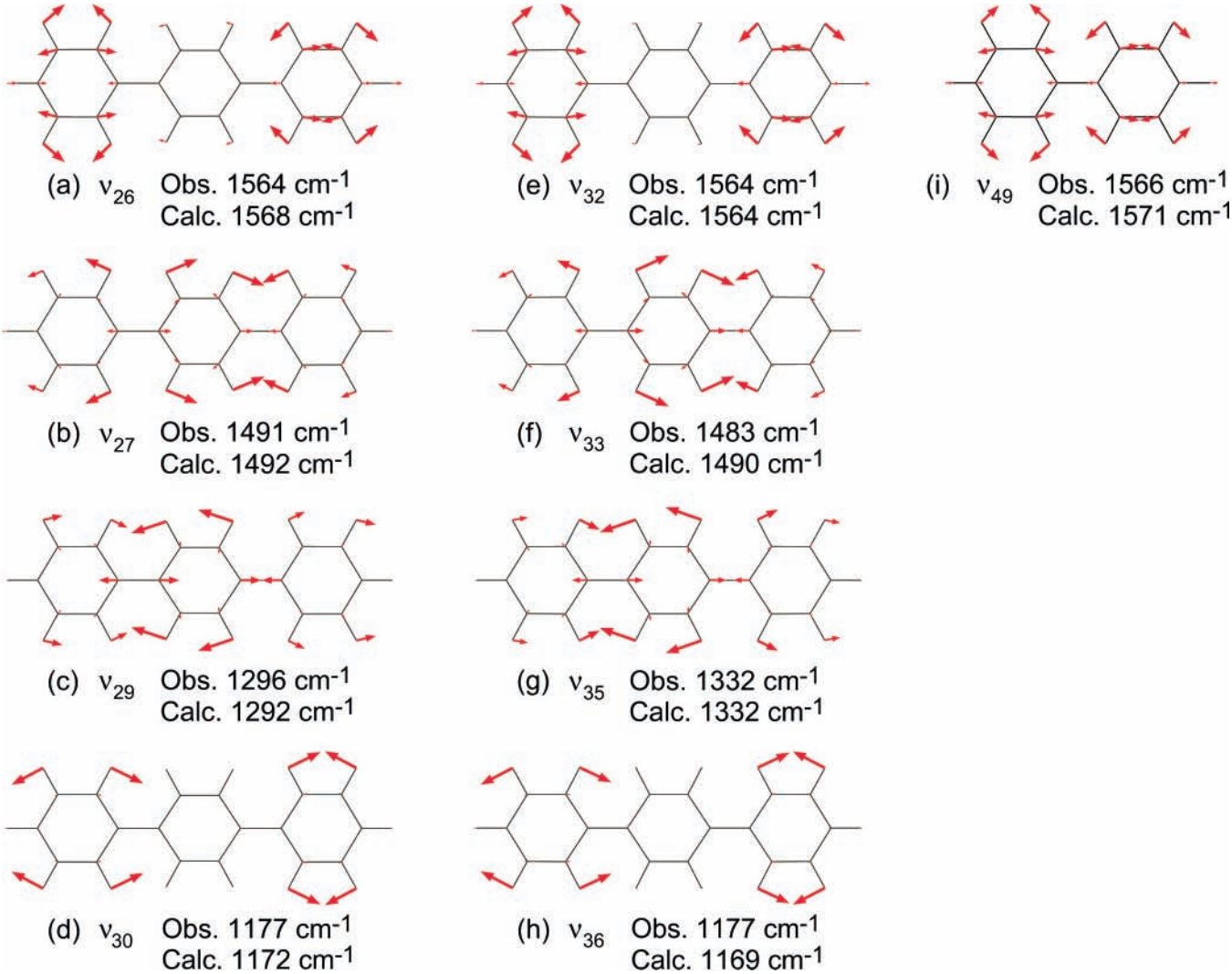

Figure 6. Atomic displacements calculated at the B3LYP/6-311+G** level for (a−d) some of the a_u modes of the *p*-terphenyl radical anion with the alternately twisted conformation, (e−h) some of the b_{1u} modes of the *p*-terphenyl dianion, and (i) one of the b_{1u} modes of the biphenyl radical anion.

Transition dipole moments associated with the a_u modes of the twisted radical anion, the b_1 modes of the helical radical anion, and the b_{1u} modes of the planar dianion are parallel to the molecular long axis (the *z*-axis in Figure 2). Similar to the spectral patterns of the radical anion (Figure 4) and dianion (Figure 5), the vibrational modes with strong infrared intensities of the radical anion (Figure 6a−d) and dianion (Figure 6e−h) also resemble each other, except for the considerable difference in wavenumber between the ν_{29} mode of the radical anion (Figure 6c) and the ν_{35} mode of the dianion (Figure 6g). These two modes can be assigned mainly to the out-of-phase inter-ring CC stretch. The upshift of the out-of-phase inter-ring CC stretch upon going from the radical anion to the dianion reflects the increasing bond order of the inter-ring C−C bonds, i.e., structural changes from benzenoid to quinoid mentioned above.

The strong infrared band observed at 1564 cm^{-1} for the radical anion (Figure 4a) corresponds to the ν_{26} mode (Figure 6a, a_u symmetry) calculated at 1568 cm^{-1} for the twisted structure (Figure 4b) and/or the ν_{27} mode (not shown, b_1 symmetry) calculated at 1567 cm^{-1} for the helical structure (Figure 4c). The strong band observed at 1564 cm^{-1} for the dianion (Figure 5a) corresponds to the ν_{32} mode (Figure 6e, b_{1u} symmetry) calculated at 1564 cm^{-1} (Figure 5b). In the ν_{26} mode of the radical anion (Figure 6a) and the ν_{32} mode of the dianion (Figure 6e), the two terminal phenyl rings change their shapes out of phase in the direction from benzenoid to quinoid. When the C_1-C_4, C_5-C_6, and C_8-C_9 bonds shrink and the C_4-C_5, C_4-C_9, C_6-C_7, and C_7-C_8 bonds stretch in the right phenyl ring, the deformation of the left phenyl ring takes place in the opposite phase. In other words, one of the phenyl rings (the right ring in Figure 6, parts a and e) changes its shape in the direction of the structural change from neutral *p*-terphenyl (benzenoid) to its radical anion and dianion (quinoid), and the other phenyl ring (the left ring in Figure 6, parts a and e) changes its shape in the opposite phase. As a result, the former ring becomes more anionic and the latter less anionic by the vibrational deformation shown in Figure 6, parts a and e. Therefore, a partial negative charge is transferred from the latter ring to the former by these vibrations. Since the charge goes back and forth as the vibration proceeds, the ν_{26} mode of the radical anion (Figure 6a) and the ν_{32} mode of the dianion (Figure 6e) generate the large dipole derivatives, namely the large transition dipole moments. The strong infrared absorption intensities associated with the ν_{26} mode of the radical anion (Figure 6a) and the ν_{32} mode of the dianion (Figure 6e) are considered to originate from the above-mentioned mechanism. This situation is closely related to that encountered in previous studies[55−62] on charged polyenes and related molecules, in which some bands in the fingerprint region have strong infrared

intensities. In those cases, the strong infrared intensities are induced by the vibrations along the bond-alternation coordinate.

The strong infrared band observed at 1491 cm^{-1} for the radical anion (Figure 4a) can be assigned to the ν_{27} mode (Figure 6b, a_u symmetry) calculated at 1492 cm^{-1} for the twisted structure (Figure 4b) and/or the ν_{28} mode (not shown, b_1 symmetry) calculated at 1493 cm^{-1} for the helical structure (Figure 4c). The strong band of the dianion at 1483 cm^{-1} (Figure 5a) corresponds to the ν_{33} mode (Figure 6f, b_{1u} symmetry) calculated at 1490 cm^{-1} (Figure 5b). In the ν_{27} mode of the radical anion (Figure 6b) and the ν_{33} mode of the dianion (Figure 6f), when the C_1-C_4 bond shrinks and the C_1-C_2, C_1-C_3, C_4-C_5, and C_4-C_9 bonds stretch around the one inter-ring C−C bond (the C_1-C_4 bond), the deformation around the other inter-ring C−C bond (the $C_{1'}-C_{4'}$ bond) takes place in the opposite phase. In other words, the $C_2C_1C_3-C_5C_4C_9$ part around the C_1-C_4 bond and the $C_{2'}C_{1'}C_{3'}-C_{5'}C_{4'}C_{9'}$ part around the $C_{1'}-C_{4'}$ bond change their shapes out of phase in the direction from benzenoid to quinoid. As a result, the $C_2C_1C_3-C_5C_4C_9$ part becomes more anionic and the $C_{2'}C_{1'}C_{3'}-C_{5'}C_{4'}C_{9'}$ part less anionic by the ν_{27} mode of the radical anion (Figure 6b) and the ν_{33} mode of the dianion (Figure 6f). Therefore, a partial negative charge goes back and forth between the right and left parts around the inter-ring C−C bonds. The large dipole derivatives along the molecular long axis induced by the ν_{27} mode of the radical anion (Figure 6b) and the ν_{33} mode of the dianion (Figure 6(f)) result in the large infrared intensities of these vibrational modes.

The ν_{29} mode of the radical anion (Figure 6c, a_u symmetry) and the ν_{35} mode of the dianion (Figure 6g, b_{1u} symmetry) correspond, respectively, to the infrared bands observed at 1296 cm^{-1} in Figure 4a and at 1330 cm^{-1} in Figure 5a. In the ν_{29} mode of the radical anion (Figure 6c) and the ν_{35} mode of the dianion (Figure 6g), when one of the inter-ring C−C bonds (the C_1-C_4 bond) shrinks, the other inter-ring C−C bond (the $C_{1'}-C_{4'}$ bond) stretches. Therefore, the charge flux between the right and left parts around the inter-ring C−C bonds is also induced by the ν_{29} mode of the radical anion (Figure 6c) and the ν_{35} mode of the dianion (Figure 6g), similar to the ν_{27} mode of the radical anion (Figure 6b) and the ν_{33} mode of the dianion (Figure 6f).

The infrared band observed at 1177 cm^{-1} for the radical anion in Figure 4a corresponds to the ν_{30} mode of the radical anion (Figure 6d, a_u symmetry) calculated at 1172 cm^{-1} for the twisted structure (Figure 4b) and/or the ν_{31} mode (not shown, b_1 symmetry) calculated at 1173 cm^{-1} for the helical structure (Figure 4c). The infrared band of the dianion observed at 1177 cm^{-1} in Figure 5a corresponds to the ν_{36} mode (Figure 6h, b_{1u} symmetry) calculated at 1169 cm^{-1} for the dianion (Figure 5b). The ν_{30} mode of the radical anion (Figure 6d) and the ν_{36} mode of the dianion (Figure 6h) are assigned mainly to the CH in-plane bending mode. However, it is noted that the ν_{30} mode of the radical anion (Figure 6d) and the ν_{36} mode of the dianion (Figure 6h) have a small contribution from the molecular symmetry coordinate, in which the right and left phenyl rings change their shapes out of phase in the direction from benzenoid to quinoid. The vibration along this molecular symmetry coordinate induces a very large dipole derivative as described above for the ν_{26} mode of the radical anion (Figure 6a) and ν_{32} mode of the dianion (Figure 6e). Therefore, in spite of the small contribution of this molecular symmetry coordinate to the ν_{30} mode of the radical anion (Figure 6d) and the ν_{36} mode of the dianion (Figure 6h), the intensities of the ν_{30} and ν_{36} modes are considered to become large.

In order to elucidate the relationship between the infrared absorption intensity and the distance of charge flux, we compare the molar absorption coefficient of the ν_{26} mode of the radical anion of *p*-terphenyl (Figure 6a) with that of the similar ν_{49} mode of the radical anion of biphenyl (Figure 6i).[20] The molar absorption coefficient of the ν_{49} mode of biphenyl is 493 mol^{-1} dm^3 cm^{-1}, while that of the ν_{26} mode of *p*-terphenyl is 2470 mol^{-1} dm^3 cm^{-1}. If we suppose that the quantities of partial negative charges transferred between the two pheynyl rings are almost the same for the ν_{49} (Figure 6i) and ν_{26} (Figure 6a) modes on the basis of the similarity of the atomic displacements in each two phenyl rings between the two modes, then the intensity of the ν_{26} mode (Figure 6a) is considered to be about 4 times larger than that of the ν_{49} mode (Figure 6i), because the distance of charge flux induced by the ν_{26} mode is about twice longer than that by the ν_{49} mode. Actually, the molar absorption coefficient of the ν_{26} mode of *p*-terphenyl (2470 mol^{-1} dm^3 cm^{-1}) becomes about 5 times larger than that of the ν_{49} mode of biphenyl (493 mol^{-1} dm^3 cm^{-1}).

It is also worth comparing the molar absorption coefficient of the ν_{26} mode of the radical anion (Figure 6a) with that of the similar ν_{32} mode of the dianion (Figure 6e), in order to elucidate the relationship between the infrared intensity and the charge incorporated in the molecules. The molar absorption coefficients of the ν_{26} mode of the radical anion and the ν_{32} mode of the dianion are 2470 and 7820 mol^{-1} dm^3 cm^{-1}, respectively. This result indicates that the infrared intensity of the ν_{32} mode of the dianion including two excess electrons is larger than that of the ν_{26} mode of the radical anion including one excess electron.

Strong infrared absorption intensities of the radical anion and dianion may also be understood qualitatively in terms of the vibronic theory proposed in 1970 by Peticolas et al.[63] The infrared absorption intensity of a fundamental vibrational transition, $I_{g1\leftarrow g0}$, can be expressed in the harmonic approximation as[63]

$$I_{g1\leftarrow g0} \propto |\langle g1|\mu|g0\rangle|^2 \quad (1)$$

$$\langle g1|\mu|g0\rangle = \sqrt{\frac{2\hbar}{\omega}} \sum_{s\neq g} \frac{1}{E_g^{\,0} - E_s^{\,0}} \left\langle g^0 \left| \left(\frac{\partial H_e}{\partial Q}\right)_0 \right| s^0 \right\rangle \langle s^0|\mu|g^0\rangle \quad (2)$$

where H_e is the electronic Hamiltonian; μ is the dipole moment operator; $|g0\rangle$ and $|g1\rangle$ represent the vibronic wavefunctions of the ground electronic state with vibrational quantum numbers 0 and 1, respectively; Q is the normal coordinate; $|g^0\rangle$ and $|s^0\rangle$ indicate the electronic wavefunctions of the ground and excited electronic states at the equilibrium structures, respectively; $E_g^{\,0}$ and $E_s^{\,0}$ are the energies of these states; and ω is the frequency of the normal vibration. From eq 2, one can understand that the infrared intensity of a vibrational band results from the vibronic coupling between the ground and excited electronic states. Strong infrared intensities come from the electronic states satisfying the following conditions: (1) the transition energy, $E_g^{\,0} - E_s^{\,0}$, is small; (2) the matrix element of the dipole moment operator, $\langle s^0|\mu|g^0\rangle$, is large (allowed transition); (3) the matrix element of the vibronic coupling operator, $\langle g^0|(\partial H_e/\partial Q)_0|s^0\rangle$, is large.

The radical anion and dianion of *p*-terphenyl give rise to strong electronic absorption bands in the visible to near-infrared region: 11 000 and 21 600 cm^{-1} (912 and 462 nm) for the radical anion (Figure 3a) and 15 400 cm^{-1} (648 nm) for the dianion (Figure 3b). These absorption bands should be polarized parallel to the molecular long axis. On the other hand, neutral

p-terphenyl gives rise to a strong band in the ultraviolet region at 35 700 cm^{-1} (280 nm).[18] Therefore, the transition energies ($E_g^0 - E_s^0$) of the radical anion and dianion is smaller than that of the neutral species. Moreover, since the a_u modes of the radical anion and the b_{1u} modes of the dianion shown in Figure 6, parts a−d and e−h, respectively, induce the changes in the electronic structures of the radical anion and dianion, these vibrational modes are probably effective for the vibronic mixing. Therefore, the matrix elements of the vibronic coupling operator for the a_u modes of the radical anion in Figure 6a−d and the b_{1u} modes of the dianion in Figure 6e−h should be larger than those for the modes of the neutral species. The transition dipole moments associated with the a_u modes of the radical anion and the b_{1u} modes of the dianion are parallel to the molecular long axis. Thus, the strong infrared intensities of the radical anion and dianion are considered to originate from their visible to near-infrared electronic absorptions through the vibronic coupling, although further theoretical and experimental studies are required for a more quantitative analysis. Time-dependent density functional theory (TD−DFT) calculations, which will tell us the excitation energies and oscillator strengths of the transitions from the ground electronic state to the excited electronic states of the radical anion and dianion, should be useful for the analysis of the strong infrared intensities of these charged species due to the vibronic coupling.

Doped conjugated polymers give rise to infrared absorptions due to vibrational transitions and electronic absorptions in the region from visible to infrared, which are associated with high electrical conductivities.[4] Thus, studies on the intensities in the infrared absorption spectra of charged oligomers and doped polymers may lead us to a better understanding of high electrical conductivities in doped polymers.

4. Concluding Remarks

In the present study, we have carried out the infrared and electronic absorption measurements of the radical anion and dianion of *p*-terphenyl in an inert gas glovebox system. The system constructed in the present study for both infrared and electronic absorption measurements can be generally applied to the spectroscopic measurements of unstable species existing in solution such as reaction intermediates.

The structures and infrared spectra of the neutral species, radical anion, and dianion of *p*-terphenyl have been calculated by using density functional theory at the B3LYP/6-311+G** level. The specific vibrational modes with the strong infrared intensities of the radical anion and dianion of *p*-terphenyl induce the changes in the electronic structure. Such electron−vibration interactions are responsible for the generation of charge fluxes,[64] which give rise to the strong infrared intensities of the radical anion and dianion.

Acknowledgment. We thank Prof. M. Tasumi, President of Saitama University, for his interest in this work and helpful advice. We thank Prof. H. Hamaguchi of the University of Tokyo for making comments on the "vibronic coupling", which led us to find ref 63. The present work was supported in part by a Grant-in-Aid for Science Research in a Priority Area "Super-Hierarchical Structures" from the Ministry of Education, Culture, Sports, Science and Technology, Japan.

References and Notes

(1) Bozio, B.; Pecile, C. In *Spectroscopy of Advanced Materials (Advances in Spectroscopy)*; Clark, R. J. H., Hester, R. E., Eds.; John Wiley & Sons: Chichester, 1991; Vol. 19, p 1.

(2) Gussoni, M.; Castiglioni, C.; Zerbi, G. In *Spectroscopy of Advanced Materials (Advances in Spectroscopy)*; Clark, R. J. H., Hester, R. E., Eds.; John Wiley & Sons: Chichester, 1991; Vol. 19, p 251.

(3) Furukawa, Y.; Tasumi, M. In *Modern Polymer Spectroscopy*; Zerbi, G., Ed.; Wiley-VCH: Weinheim, 1999, p 207.

(4) Kiess, H., Ed. *Conjugated Conducting Polymers*; Springer-Verlag: Berlin, 1992.

(5) Su, W. P.; Schrieffer, J. R. *Proc. Natl. Acad. Sci. U.S.A.* **1980**, *77*, 5625.

(6) Brazovskiĭ, S. A.; Kirova, N. N. *Sov. Phys. JETP Lett.* **1981**, *33*, 4.

(7) Bishop, A. R.; Campbell, D. K.; Fesser, K. *Mol. Cryst. Liq. Cryst.* **1981**, *77*, 253.

(8) Brédas, J. L.; Chance, R. R.; Silbey, R. *Mol. Cryst. Liq. Cryst.* **1981**, *77*, 319.

(9) Brédas, J. L.; Themans, B.; Fripiat, J. G.; André, J. M.; Chance, R. R. *Phys. Rev. B* **1984**, *29*, 6761.

(10) Cuff, L.; Cui, C.; Kertesz, M. *J. Am. Chem. Soc.* **1994**, *116*, 9269.

(11) Ehrendorfer, Ch.; Karpfen, A. *J. Phys. Chem.* **1995**, *99*, 10196.

(12) Irle, S.; Lischka, H. *J. Chem. Phys.* **1995**, *103*, 1508.

(13) Irle, S.; Lischka, H. *J. Chem. Phys.* **1997**, *107*, 3021.

(14) Rubio, M.; Merchán, M.; Ortí, E.; Roos, B. O. *J. Phys. Chem.* **1995**, *99*, 14980.

(15) Furuya, K.; Torii, H.; Furukawa, Y.; Tasumi, M. *Chem. Lett.* **1996**, 913.

(16) Furuya, K.; Torii, H.; Furukawa, Y.; Tasumi, M. *J. Mol. Struct. (Theochem)* **1998**, *424*, 225.

(17) Honda, K.; Furukawa, Y.; Furuya, K.; Torii, H.; Tasumi, M. *J. Phys. Chem. A* **2002**, *106*, 3587.

(18) Furukawa, Y.; Ohtsuka, H.; Tasumi, M. *Synth. Met.* **1993**, *55*, 516.

(19) Furukawa, Y.; Ohtsuka, H.; Tasumi, M.; Wataru, I.; Kanbara, T.; Yamamoto, T. *J. Raman Spectrosc.* **1993**, *24*, 551.

(20) Sakamoto, A.; Kuroda, M.; Harada, T.; Tasumi, M. *J. Mol. Struct.* **2005**, *735*−736, 3.

(21) Kachkurova, I. Ya. *Dokl. Akad. Nauk S. S. S. R.* **1965**, *163*, 1198.

(22) Kachkurova, I. Ya. *Teor. Eksp. Khim.* **1967**, *3*, 498.

(23) Dodson, C. L.; Graham, J. F. *J. Phys. Chem.* **1973**, *77*, 2903.

(24) Juchnovski, I.; Kolev, Ts.; Rashkov, I. *Spectrosc. Lett.* **1985**, *18*, 171.

(25) Eargle, D. H., Jr. *J. Org. Chem.* **1970**, *35*, 3744.

(26) Torii, H.; Ueno, Y.; Sakamoto, A.; Tasumi, M. *Can. J. Chem.* **2004**, *82*, 951.

(27) Bewick, A.; Pons, S. In *Advances in Infrared and Raman Spectroscopy*; Clark, R. J. H.; Hester, R. E. Eds.; John Wiley & Sons: Chichester, 1985; Vol. 12, p 1.

(28) Szczepanski, J.; Roser, D.; Personette, W.; Eyring, M.; Pellow, R.; Vala, M. *J. Phys. Chem.* **1992**, *96*, 7876.

(29) Szczepanski, J.; Vala, M.; Talbi, D.; Parisel, O.; Ellinger, Y. *J. Chem. Phys.* **1993**, *98*, 4494.

(30) Szczepanski, J.; Chapo, C.; Vala, M. *Chem. Phys. Lett.* **1993**, *205*, 434.

(31) Szczepanski, J.; Vala, M. *Nature (London)* **1993**, *363*, 699.

(32) Vala, M.; Szczepanski, J.; Pauzat, F.; Parisel, O.; Talbi, D.; Ellinger, Y. *J. Phys. Chem.* **1994**, *98*, 9187.

(33) Szczepanski, J.; Wehlburg, C.; Vala, M. *Chem. Phys. Lett.* **1995**, *232*, 221.

(34) Szczepanski, J.; Drawdy, J.; Wehlburg, C.; Vala, M. *Chem. Phys. Lett.* **1995**, *245*, 539.

(35) Hudgins, D. M.; Sandford, S. A.; Allamandola, L. J. *J. Phys. Chem.* **1994**, *98*, 4243.

(36) Hudgins, D. M.; Allamandola, L. J. *J. Phys. Chem.* **1995**, *99*, 3033.

(37) Hudgins, D. M.; Allamandola, L. J. *J. Phys. Chem.* **1995**, *99*, 8978.

(38) Hudgins, D. M.; Allamandola, L. J. *J. Phys. Chem. A* **1997**, *101*, 3472.

(39) Szczepanski, J.; Personette, W.; Vala, M. *Chem. Phys. Lett.* **1991**, *185*, 324.

(40) Szczepanski, J.; Personette, W.; Pellow, R.; Chandrasekhar, T. M.; Roser, D.; Cory, M.; Zerner, M.; Vala, M. *J. Chem. Phys.* **1992**, *96*, 35.

(41) Tang, W.; Zhang, X.-L.; Bally, T. *J. Phys. Chem.* **1993**, *97*, 4373.

(42) Devlin, J. P.; Mckennis, J. S.; Thornton, C.; Moore, J. C. *J. Phys. Chem.* **1982**, *86*, 2613.

(43) Manceron, L.; Andrews, L. *J. Am. Chem. Soc.* **1988**, *110*, 3840.

(44) Becke, A. D. *J. Chem. Phys.* **1993**, *98*, 5648.

(45) Lee, C.; Yang, W.; Parr, R. G. *Phys. Rev. B* **1988**, *37*, 785.

(46) Frisch, M. J.; Trucks, G. W.; Schlegel, H. B.; Scuseria, G. E.; Robb, M. A.; Cheeseman, J. R.; Montgomery, J. A., Jr.; Vreven, T.; Kudin, K. N.; Burant, J. C.; Millam, J. M.; Iyengar, S. S.; Tomasi, J.; Barone, V.; Mennucci, B.; Cossi, M.; Scalmani, G.; Rega, N.; Petersson, G. A.; Nakatsuji, H.; Hada, M.; Ehara, M.; Toyota, K.; Fukuda, R.; Hasegawa, J.; Ishida, M.; Nakajima, T.; Honda, Y.; Kitao, O.; Nakai, H.; Klene, M.; Li, X.; Knox, J. E.; Hratchian, H. P.; Cross, J. B.; Adamo, C.; Jaramillo, J.; Gomperts, R.; Stratmann, R. E.; Yazyev, O.; Austin, A. J.; Cammi, R.; Pomelli, C.; Ochterski, J. W.; Ayala, P. Y.; Morokuma, K.; Voth, G. A.;

Salvador, P.; Dannenberg, J. J.; Zakrzewski, V. G.; Dapprich, S.; Daniels, A. D.; Strain, M. C.; Farkas, O.; Malick, D. K.; Rabuck, A. D.; Raghavachari, K.; Foresman, J. B.; Ortiz, J. V.; Cui, Q.; Baboul, A. G.; Clifford, S.; Cioslowski, J.; Stefanov, B. B.; Liu, G.; Liashenko, A.; Piskorz, P.; Komaromi, I.; Martin, R. L.; Fox, D. J.; Keith, T.; Al-Laham, M. A.; Peng, C. Y.; Nanayakkara, A.; Challacombe, M.; Gill, P. M. W.; Johnson, B.; Chen, W.; Wong, M. W.; Gonzalez, C.; Pople, J. A. *Gaussian 03*, revision C.02; Gaussian Inc.: Wallingford, CT, 2004.

(47) Okamoto, Y. *VLX*; Fuji Photo Film Co.Ltd, 2003.

(48) Honda, K.; Furukawa, Y. *J. Mol. Struct.* **2005**, *735*−736, 11.

(49) Baudour, J. L.; Cailleau, H.; Yelon, W. B. *Acta Crystallogr.* **1977**, *B33* 1773.

(50) Baudour, J. L.; Delugeard, Y.; Cailleau, H. *Acta Crystallogr.* **1976**, *B32*, 150.

(51) Rietveld, H. M.; Maslen, E. N.; Clews, C. J. B. *Acta Crystallogr.* **1970**, *B26*, 693.

(52) Murakami, J.; Okuyama, K.; Ito, M. *Bull. Chem. Soc. Jpn.* **1982**, *55*, 3422.

(53) Balk, P.; Hoijtink, G. J.; Schreurs, J. W. H. *Recl. Trav. Chim. Pays-Bas* **1957**, *76*, 813.

(54) Nakanishi, K.; Solomon, P. H. *Infrared Absorption Spectroscopy*; Emerson Adams Press Inc: Boca Raton, FL, 1998.

(55) Fincher, C. R., Jr.; Ozaki, M.; Heeger, A. J.; MacDiarmid, A. G. *Phys. Rev. B* **1979**, *19*, 4140.

(56) Harada, I.; Furukawa, Y.; Tasumi, M.; Shirakawa, H.; Ikeda, S. *J. Chem. Phys.* **1980**, *73*, 4746.

(57) Piaggio, P.; Dellepiane, D.; Piseri, L.; Tubino, R.; Taliani, C. *Solid State Commun.* **1984**, *50*, 947.

(58) Masuda, S.; Torii, H.; Tasumi, M. *J. Phys. Chem.* **1996**, *100*, 15335.

(59) Torii, H.; Tasumi, M.; *J. Phys. Chem. B* **1997**, *101*, 466.

(60) Furuya, K.; Inagaki, Y.; Torii, H.; Furukawa, Y.; Tasumi, M. *J. Phys. Chem. A* **1998**, *102*, 8413.

(61) Torii, H.; Furuya, K.; Tasumi, M. *J. Phys. Chem. A* **1998**, *102*, 8422.

(62) Furuya, K.; Torii, H.; Furukawa, Y.; Tasumi, M. *J. Phys. Chem. A* **2000**, *104*, 11203.

(63) Peticolas, W. L.; Nafie, L.; Stein, P.; Fanconi, B. *J. Chem. Phys.* **1970**, *52*, 1576.

(64) Torii, H.; Ueno, Y.; Sakamoto, A.; Tasumi, M. *J. Phys. Chem. A* **1999**, *103*, 5557.